Octupolar versus Néel Order in Cubic 5d^{2} Double Perovskites

D. D. Maharaj, G. Sala, M. B. Stone, E. Kermarrec, C. Ritter, F. Fauth, C. A. Marjerrison, J. E. Greedan, A. Paramekanti, and B. D. Gaulin

Octupolar vs Néel Order in Cubic $5d^2$ double perovskites

D. D. Maharaj,[1, *] G. Sala,[1, 2] M. B. Stone,[2] E. Kermarrec,[1, 3] C. Ritter,[4] F. Fauth,[5]
C. A. Marjerrison,[6] J. E. Greedan,[6, 7] A. Paramekanti,[8] and B. D. Gaulin[1, 6, 9]

[1]*Department of Physics and Astronomy, McMaster University, Hamilton, ON L8S 4M1 Canada*
[2]*Neutron Scattering Division, Oak Ridge National Laboratory, Oak Ridge, Tennessee 37831, USA*
[3]*Laboratoire de Physique des Solides, CNRS, Univ. Paris-Sud,*
Université Paris-Saclay, 91405 Orsay Cedex, France
[4]*Institut Laue-Langevin, Boîte Postale 156, 38042 Grenoble Cédex, France*
[5]*CELLS-ALBA Synchrotron, Carrer de la Llum 2-26, 08290 Cerdanyola del Vallès, Barcelona, Spain*
[6]*Brockhouse Institute for Materials Research, McMaster University, Hamilton, ON L8S 4M1 Canada*
[7]*Department of Chemistry and Chemical Biology, McMaster University, ON, L8S 4M1, Canada*
[8]*Department of Physics, University of Toronto, 60 St. George Street, Toronto, ON, M5S 1A7 Canada*
[9]*Canadian Institute for Advanced Research, 661 University Ave., Toronto, ON M5G 1M1 Canada*
(Dated: January 30, 2020)

We report time-of-flight neutron spectroscopy, and neutron and X-ray diffraction studies, of the $5d^2$ double perovskite (DP) magnets, Ba_2MOsO_6 (M = Zn, Mg, Ca). These materials host antiferromagnetically coupled $5d^2$ Os^{6+} ions decorating a face-centred cubic (FCC) lattice, and are found to remain cubic down to the lowest temperatures. They all exhibit thermodynamic anomalies consistent with a single phase transition at a temperature T^*, and a gapped magnetic excitation spectrum with spectral weight concentrated at wavevectors typical of type-I antiferromagnetic orders. However, while muon spin resonance experiments show clear evidence for time-reversal symmetry breaking below T^*, we observe no corresponding magnetic Bragg scattering signal. These results are shown to be consistent with ferro-octupolar symmetry breaking below T^*, and are discussed in the context of other $5d$ DP magnets, and theories of exotic orders driven by multipolar interactions.

Introduction — Ordered double perovskite (DP) magnets, with the chemical formula $A_2BB'O_6$, provide a fascinating avenue to study the interplay of geometric frustration with strong spin-orbit coupling (SOC) [1]. Here, B and B' sublattices individually form an FCC lattice of edge-sharing tetrahedra, an archetype for geometric frustration in three dimensions. Furthermore, the flexibility of the DP lattice to host heavy ions at the B' site allows the study of spin-orbit driven physics, as the strength of SOC scales $\sim Z^2$, where Z is the atomic number of the magnetic ion [2]. This interplay of SOC and frustration in DPs is predicted to yield exotic ground states [3–6].

The single-particle t_{2g} levels in an octahedral crystal field are split by strong SOC, resulting in a quartet $j = 3/2$ ground state and a doublet $j = 1/2$ excited state. Famously, for a d^5 electronic configuration, as occurs for Ir^{4+} or Ru^{3+}, this results in a single $j = 1/2$ hole, leading to extreme quantum magnetism, and Kitaev exchange interactions in appropriate geometries [7–13]. On the other hand, ions with d^1 and d^2 configurations are respectively expected to form $j = 3/2$ or total $J = 2$ moments [3, 4, 6]. Theoretical studies incorporating intersite orbital repulsion between such ions argue for wide regimes of quadrupolar order on the FCC lattice [3, 4, 6] which may coexist with dipolar antiferromagnetic (AF) or valence bond orders [14]. Recent experiments on $5d^1$ oxides, Ba_2NaOsO_6 with Os^{7+} [15, 16] and Ba_2MgReO_6 with Re^{6+} [17], have found evidence for two transitions associated with these distinct broken symmetries: quadrupolar

ordering at T_Q and onset of coexisting dipolar AF order below a lower transition temperature T_N.

In this Letter, we explore the case of d^2 ions on the B' site, with effective $J = 2$ moments. We report new magnetic neutron powder diffraction (NPD), inelastic neutron scattering (INS), and high angular resolution synchrotron X-ray diffraction (XRD) results on three cubic DPs: Ba_2MOsO_6, with M = Zn, Mg, Ca (respectively referred to henceforth as BZO, BMO, and BCO). In contrast to d^1 DPs, these materials display clear thermodynamic signatures of a *single* phase transition [18–20] at $T^* \sim$ 30-50 K, which is associated with time-reversal symmetry breaking based on oscillations observed in zero field muon spin relaxation (ZF-μSR) [20]. Our INS results show strong, gapped, magnetic spectral weight at wavevectors typical of type-I AF order, but we detect *no clear signature of an ordered AF moment* in the diffraction data, leading us to place an upper limit between 0.13-0.06 μ_B per B' site. Furthermore, our NPD and XRD results show *no deviation from cubic symmetry*, thus ruling out quadrupolar order. We propose that these striking and unexpected results may be understood via the emergence of time-reversal symmetry breaking ferro-octupolar order below T^*.

Multipolar orders have been extensively studied in heavy fermion f-electron compounds [21]. Examples include NpO_2 [22–25], where experiments suggest a primary rank-5 magnetic multipolar order driving secondary quadrupolar order, the "hidden order" state of URu_2Si_2

[26–28], and recent discoveries of quadrupolar and octupolar orders in PrX_2Al_{20} (X = Ti, V) [29–31]. In stark contrast, multipolar orders in d-electron systems are less explored [15–17, 32–34]; our work appears to be the first reported candidate for d-orbital octupolar order.

BZO, BMO and BCO have been previously studied in powder form. In all three materials, NPD and XRD confirm that they remain in the cubic $Fm\bar{3}m$ space group down to the lowest temperature. They all display Curie-Weiss-like magnetic susceptibilities (χ) at high temperatures, with large AF Curie-Weiss constants ($\Theta_{CW} \sim 130$ K), and anomalies at T^* in the form of a splitting between field-cooled and zero-field cooled results. They all exhibit peaks in their heat capacity, or in the related measure $d(\chi T)/dT$, at $T^* \sim 50$ K (BMO, BCO) or $T^* \sim 30$ K (BZO), indicating a phase transition [18, 20]. These findings are summarized in Table I.

The entropy released up to $\sim 2T^*$ in all three materials appears to be $\sim R\ln(2)$ per mole, as explicitly shown for BZO and BMO in the Supplemental Material (SM)[35, 36]. This is much smaller than the $R\ln(5)$ expected for an effective $J = 2$ moment [18–20], and it points to part of the entropy being quenched at $T \gg T^*$ (i.e., above ~ 200 K). This is in contrast to the $\sim R\ln(5)$ entropy released up to $\sim 2T_N$ for the tetragonal counterpart Sr_2MgOsO_6, which has a high Néel ordering temperature $T_N \sim 100$ K [37].

These three cubic samples have also been previously studied using μSR techniques [18, 20], and it is primarily on the basis of these zero longitudinal field μSR oscillations for $T < T^*$, indicative of a time-reversal broken state, that the transition at T^* was associated with AF order. However, no magnetic neutron diffraction peaks could be identified in this earlier study at low temperatures, with a sensitivity to ordered moment of ~ 0.7 μ_B. In the present work, we *significantly* improve on this bound, still finding no evidence of magnetic Bragg peaks.

The corresponding $5d^3$ osmium-based DPs, both cubic Ba_2YOsO_6 and monoclinic Sr_2ScOsO_6 and La_2LiOsO_6, show clear Néel transitions to AF ordered states, with large ordered moments $\sim 1.7\mu_B$ [19, 38–41]. These observed ordered moments are reduced from the $3\mu_B$ value

expected for an orbitally-quenched moment, pointing to strong SOC effects, or covalency, or both. Nonetheless magnetic Bragg scattering at the (100) and (110) positions is easily observed, along with strong, gapped inelastic magnetic scattering centred at these two ordering wavevectors. Previously studied $5d^2$ DPs such as monoclinic Sr_2MgOsO_6 and cubic Ba_2LuReO_6 (with Re^{5+}) also show transitions to Type I AF order, as seen via neutron diffraction, albeit with much smaller ordered moments, 0.6(2) and 0.34(4) μ_B, respectively [37, 42].

Below we present our experimental findings on powder samples of the cubic systems, BZO, BMO and BCO. Details of experimental and analysis methods are in the SM [35], which includes Refs. [43–47]. Our new NPD measurements on D20 [48] at the Institut Laue Langevin (ILL) have ~ 10 to 20 times more sensitivity to magnetic Bragg scattering as compared with previous NPD measurements taken at the C2 instrument of the Chalk River Laboratories. No magnetic Bragg scattering is observed at 10 K, factors of 3–5 below T^* for any of these materials. We do however observe gapped, inelastic magnetic spectral weight centred on wavevectors characteristic of type-I AF order. We thus conclude that the dominant broken symmetry below T^* in these three cubic DP d^2 magnets must involve multipolar ordering.

Results – Time-of-flight INS measurements from SEQUOIA [49] are shown in Fig.1. Panels (a)-(c) show the INS spectra well below (top panel) and above T^* for BZO, BMO, and BCO respectively. Panels (d)-(f) show cuts through this data as a function of energy, integrating all $|Q| < 1.15$ Å^{-1} and as a function of temperature, again for BZO, BMO and BCO respectively.

The data sets for all three samples in Fig. 1 are similar, with gapped magnetic spectral weight at low $|Q|$'s, typical of the 100 (0.78 Å^{-1}) and 110 (1.1 Å^{-1}) Bragg positions. The full bandwidth of the magnetic excitation spectrum appears to be ~ 6 meV. From Fig. 1 b), c), e), and f), this magnetic spectral weight overlaps in energy with strong phonon scattering near ~ 18 meV and 14 meV for BMO and BCO respectively. Even though our low $|Q|$-integration favours magnetic scattering at the expense of scattering from phonons, whose intensity tends to go like $|Q|^2$, we still pick up a sizeable contribution from this high phonon density of states (DOS), especially at high temperatures where the thermal population of the phonons is large. The observed redshift in the peak of the phonon DOS from ~ 17 meV in BMO to ~ 14 meV for BCO is expected since Ca^{2+} is isoelectronic to Mg^{2+} but heavier. While the Zn^{2+} in BZO is heavier still than Ca^{2+}, it is not isoelectronic, instead possessing a filled $3d$ shell. This might lead to its higher energy phonon.

As the high phonon DOS is well separated from the magnetic spectral weight in BZO, shown in Figs. 1(a) and 1(d), this is where the nature of the gapped magnetic scattering is most easily appreciated. The energy cuts in Fig. 1(d) clearly show a well developed gap of $\sim$

System	T^*	θ_{CW}	a (Å)	Ref.	μ_{ord}
Ba_2CaOsO_6	49	−156.2(3)	8.3456	[13]	$< 0.11\mu_B$
Ba_2MgOsO_6	51	−120(1)	8.0586	[15]	$< 0.13\mu_B$
Ba_2ZnOsO_6	30	−149.0(4)	8.0786	[15]	$< 0.06\mu_B$

TABLE I. Summary of experimental results for the three cubic DPs studied. T^* denotes the peak in the heat capacity indicating a thermodynamic phase transition [18, 20]. θ_{CW} is the Curie-Weiss temperature extracted from high temperature susceptibility data [18, 20]. μ_{ord} is the upper limit on the ordered dipolar moment associated with type-I AF order, as determined from neutron diffraction in this work.

10 meV and a bandwidth of ~ 6 meV. This structure collapses by 25 K, where $T^* = 30$ K for BZO, at which point the gap has largely filled in and only a vestige of an overdamped spin excitation at ~ 10 meV remains. This is very similar to what occurs in the d^3 DPs on the approach to their T_Ns, *except* that there is no obvious temperature dependent Bragg scattering at the 100 or 110 positions, as would be expected for type-I AF order.
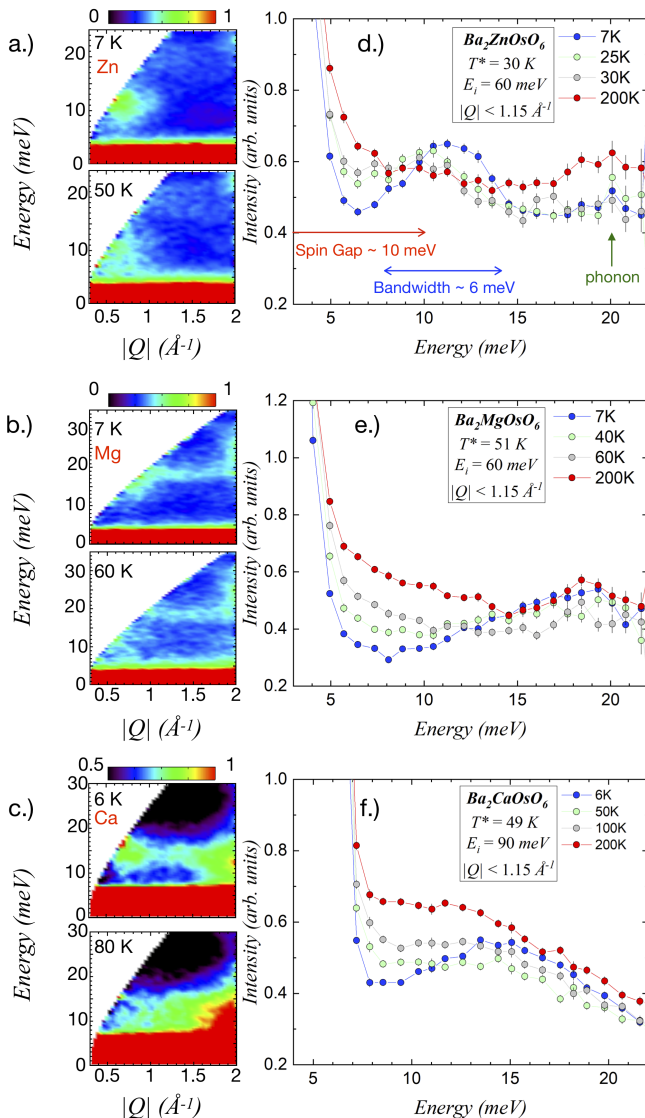

FIG. 1. (a) - (c): Neutron scattering intensity contour plots for BZO, BMO, and BCO shown as a function of energy transfer, E and momentum transfer $|Q|$ at base temperature (top) and at $T > T^*$ (bottom), respectively. Below T^*, clear gapped magnetic inelastic spectral weight develops around (100) and (110) wavevectors (~ 0.78 Å^{-1}) and 110 (1.1 Å^{-1}) in each case. (d) and (e): Low $|Q|$ integrated cuts of the neutron scattering intensity as a function of energy transfer E as a function of temperature for BZO, BMO, and BCO, respectively. A gap in the magnetic excitation spectrum is clearly revealed for each compound for $T < T^*$.
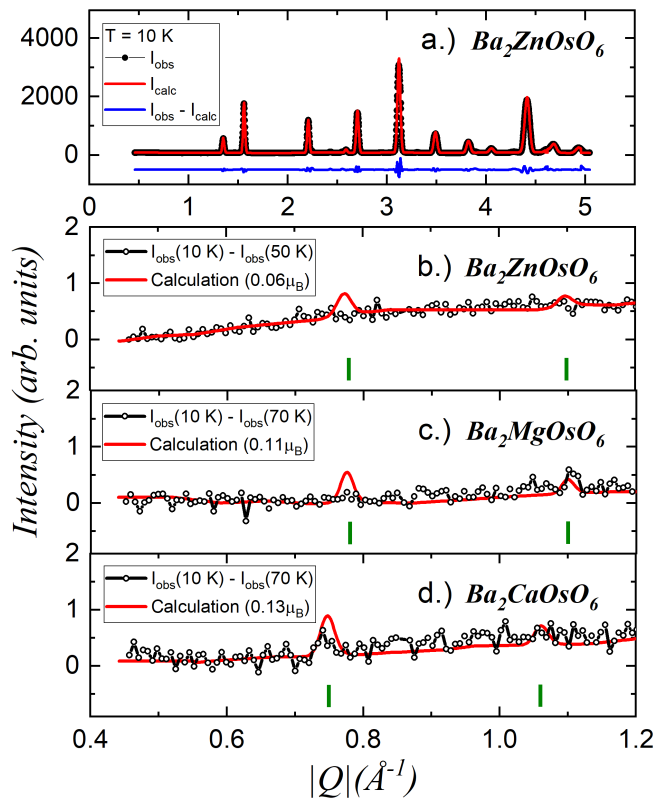

FIG. 2. (a) NPD measurements on BZO for $T = 10$ K with the experimental data set in black and the fit to the refined $Fm\bar{3}m$ structure in red. (b) Subtraction of the 50 K data set from the 10 K data set. The red line shows the calculated magnetic diffraction pattern for BZO with an Os^{6+} ordered moment of $0.06\mu_B$, which we establish as the upper limit for an ordered dipole moment in BZO . Green fiducial lines indicate the locations of the magnetic peaks expected for type-I AF order. Panels (c) and (d) show the same comparison for BMO and BCO. These establish upper limits on an ordered Os^{6+} dipole moment of $0.11\mu_B$ and $0.13\mu_B$, respectively.

The absence of evidence for magnetic Bragg scattering is seen in Fig. 2. Fig. 2(a) shows neutron diffraction data taken at T = 10 K, well below $T^* = 30$ K in BZO, using the D20 diffractometer at the ILL [48]. This data and the corresponding NPD data on BMO and BCO refine in the cubic $Fm\bar{3}m$ space group at all temperatures measured. Figure 2 b), c) and d) then show a subtraction of high temperature (50 K for BZO; 70 K for BMO and BCO) data sets from low temperature data sets for each of BZO, BCO, and BMO, respectively. A calculated neutron diffraction profile appropriate for a type-I AF structure below T^* is shown as the red line in Fig. 2 b), c) and d), where the assumed ordered moment in the calculation is $0.06\mu_B$ for BZO (b), $0.11\mu_B$ for BMO (c), and $0.13\mu_B$ for BCO (d). Taking the case where the evidence *against* long range magnetic order below T^* is most stringent, BZO, we can eliminate conventional type-I AF order of magnetic dipoles with an ordered moment
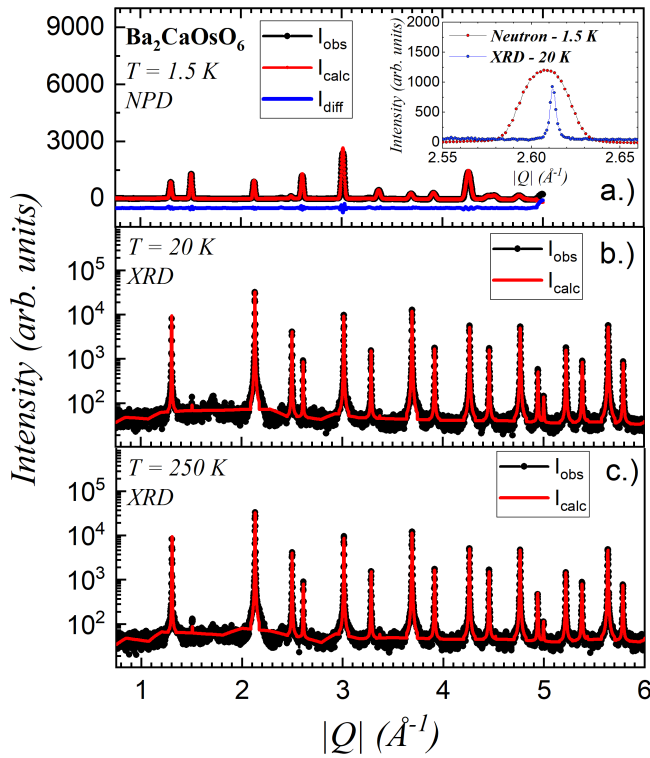
FIG. 3. (a) The NPD profile for BCO is shown at $T = 1.5$ K in the main panel, while the inset shows a comparison of NPD vs synchrotron XRD data taken on BCO at 20 K. Panels (b) and (c) show synchrotron XRD data on BCO at T = 20 K (b), and T = 250 K (c), along with corresponding cubic structural refinements, in red.

greater than $\sim 0.06\mu_B$. This upper limit for magnetic dipole order is a factor of ~ 12 more stringent than previous limits on magnetic Bragg scattering for this family of cubic DP materials. This upper bound for $\mu_{\rm ord}$ in BCO is $\sim 35\%$ lower than the value, $0.2\mu_B$, previously extracted from a comparison of the μSR internal fields of BCO and Ba_2YRuO_6 [18, 50].

Competing multipolar orders. — Our study shows all or most of the static $5d^2$ moment of Os^{6+} in BZO, BMO and BCO is not visible to neutron diffraction below T^*. Nonetheless, strong inelastic magnetic scattering is easily observed at all temperatures, and it is most clearly gapped at $T \ll T^*$. One scenario to explain these results is that the ground state has dominant quadrupolar ordering, accompanied by weak dipolar ordering [3, 4, 6]. A quadrupolar ordering transition at $T \gg T^*$ can partially quench the $R\ln(5)$ entropy, with the residual $\sim R\ln(2)$ entropy being quenched by AF dipolar ordering at T^* which breaks time-reversal symmetry. The quadrupolar order can also pin the direction of the ordered dipole moment, explaining the spin-gap, and if the ordered dipole moment is weak, it may escape detection in a NPD experiment. However, the orbital selection accompanying such a quadrupolar order would lower the crystal symmetry, at odds with our high resolution NPD data shown for BCO in Fig. 2(a). We have carried out even higher resolution XRD measurements on BCO, the family member which best exhibits undamped ZF-μSR oscillations. These measurements were conducted at the high angular resolution diffraction instrument $BL04 - MSPD$, beamline 8 of the ALBA Synchrotron Light facility (Barcelona, Spain) [51]. The sensitivity of these measurements to possible weak splittings of the cubic Bragg peaks is ~ 10 times greater than the NPD measurements; see Fig. 3(a) inset. These XRD results, in Figs. 3 (b)-(d), show no splitting or broadening of the cubic Bragg peaks, yielding an upper limit on local distortions $< 0.1\%$ (see SM [35]). This confirms that BCO remains cubic even for $T \ll T^*$, ruling out quadrupolar ordering. We contrast this with the $5d^1$ osmate Ba_2NaOsO_6 which exhibits measurable $\sim 0.5\%$-0.7% local distortions associated with quadrupolar ordering [52].

Here, we propose a distinct scenario, an octupolar ordered ground state, that provides the most promising vehicle to explain all the salient observations. For an effective $J = 2$ moment, a residual octahedral crystal field Hamiltonian is $H_{\rm CEF'} = -V_{\rm eff}(\mathcal{O}_{40} + 5\mathcal{O}_{44})$, where the Steven's operators (dropping constant terms) are

$$\mathcal{O}_{40} = 35J_z^4 - (30J(J+1) - 25)J_z^2 \qquad (1)$$

$$\mathcal{O}_{44} = \frac{1}{2}(J_+^4 + J_-^4). \qquad (2)$$

$V_{\rm eff} > 0$ results in a non-Kramers ground state doublet and an excited triplet with a gap $\Delta = 120V_{\rm eff}$, as shown in Fig. 4 (details in SM [35]). This naturally accounts for partial entropy quenching for $T \lesssim \Delta$, without a phase transition, with the residual $R\ln(2)$ entropy being quenched by ordering within the doublet sector at T^*. In the $|J_z = m\rangle$ basis, the ground state wavefunctions are $|\psi_{g,\uparrow}\rangle = |0\rangle$ and $|\psi_{g,\downarrow}\rangle = \frac{1}{\sqrt{2}}(|2\rangle + |-2\rangle)$, with excited triplet wavefunctions $|\psi_{e,\pm}\rangle = |\pm 1\rangle$ and $|\psi_{e,0}\rangle = \frac{1}{\sqrt{2}}(|2\rangle - |-2\rangle)$. The ground state manifold has vanishing matrix elements for the dipole operators $\vec{J}$, precluding dipolar order. However, $\vec{J}$ can induce
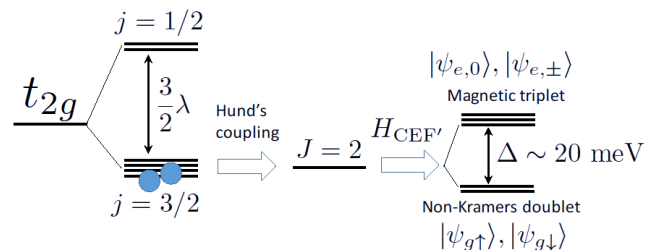

FIG. 4. Schematic level diagram showing single-particle t_{2g} orbitals split by SOC (λ) and interactions (Hund's coupling) leading to a $J = 2$ ground state. Residual crystal field $H_{\rm CEF'}$ splits this $J = 2$ manifold into a non-Kramers doublet ground state and an excited magnetic triplet (see text for details).

transitions into the excited triplet, accounting for the spin gap in INS. Defining pseudospin-1/2 operators $\vec{\tau}$ within the ground doublet, the quadrupolar operators are $(J_x^2 - J_y^2) \equiv 2\sqrt{3}\tau_x$, $(3J_z^2 - J^2) \equiv -6\tau_z$, while the octupolar operator $\overline{J_x J_y J_z} \equiv -\sqrt{3}\tau_y$ (overline denoting symmetrization). Octupolar order, with $\langle\tau_y\rangle \neq 0$, leads to broken time-reversal symmetry below T^* while preserving cubic symmetry. A mean field calculation with $\langle\tau_y\rangle \neq 0$ qualitatively captures the observed entropy and magnetic susceptibility (see SM [35]). Further implications of this proposal are studied in Ref. [53].

To conclude, the low temperature phases of the cubic $5d^2$ DPs BZO, BMO, and BCO are best described arising from octupolar order within a non-Kramers ground state doublet. This exotic ground state appears to require the perfect FCC structure as non-cubic d^2 DPs, such as Sr_2MgOsO_6 [37], where the non-Kramers degeneracies are broken and AF exchange is stronger, display conventional AF ground states. Further structural studies, using dilatometry and total X-ray scattering on single crystals, and probes such as magnetostriction or Raman scattering [54], may provide smoking gun signatures of octupolar order in these $5d^2$ materials.

ACKNOWLEDGMENTS

* maharadd@mcmaster.ca

[1] W. Witczak-Krempa, G. Chen, Y. B. Kim, and L. Balents, Annual Review of Condensed Matter Physics **5**, 57 (2014).

[2] K. V. Shanavas, Z. S. Popović, and S. Satpathy, Phys. Rev. B **90**, 165108 (2014).

[3] G. Chen, R. Pereira, and L. Balents, Phys. Rev. B **82**, 174440 (2010).

[4] G. Chen and L. Balents, Phys. Rev. B **84**, 094420 (2011).

[5] C. Svoboda, M. Randeria, and N. Trivedi, Phys. Rev. B **95**, 014409 (2017).

[6] C. Svoboda, M. Randeria, and N. Trivedi, arXiv e-prints , arXiv:1702.03199 (2017), arXiv:1702.03199 [cond-mat.str-el].

[7] J. c. v. Chaloupka, G. Jackeli, and G. Khaliullin, Phys. Rev. Lett. **105**, 027204 (2010).

[8] Y. Singh, S. Manni, J. Reuther, T. Berlijn, R. Thomale, W. Ku, S. Trebst, and P. Gegenwart, Phys. Rev. Lett. **108**, 127203 (2012).

[9] K. W. Plumb, J. P. Clancy, L. J. Sandilands, V. V. Shankar, Y. F. Hu, K. S. Burch, H.-Y. Kee, and Y.-J. Kim, Phys. Rev. B **90**, 041112 (2014).

[10] S. Hwan Chun, J.-W. Kim, J. Kim, H. Zheng, C. C. Stoumpos, C. D. Malliakas, J. F. Mitchell, K. Mehlawat, Y. Singh, Y. Choi, T. Gog, A. Al-Zein, M. M. Sala, M. Krisch, J. Chaloupka, G. Jackeli, G. Khaliullin, and B. J. Kim, Nature Physics **11**, 462 EP (2015).

[11] A. Banerjee, C. A. Bridges, J. Q. Yan, A. A. Aczel, L. Li, M. B. Stone, G. E. Granroth, M. D. Lumsden, Y. Yiu, J. Knolle, S. Bhattacharjee, D. L. Kovrizhin, R. Moessner, D. A. Tennant, D. G. Mandrus, and S. E. Nagler, Nature Materials **15**, 733 EP (2016).

[12] S. M. Winter, A. A. Tsirlin, M. Daghofer, J. van den Brink, Y. Singh, P. Gegenwart, and R. Valentí, Journal of Physics: Condensed Matter **29**, 493002 (2017).

[13] Y. Kasahara, T. Ohnishi, Y. Mizukami, O. Tanaka, S. Ma, K. Sugii, N. Kurita, H. Tanaka, J. Nasu, Y. Motome, T. Shibauchi, and Y. Matsuda, Nature **559**, 227 (2018).

[14] J. Romhányi, L. Balents, and G. Jackeli, Phys. Rev. Lett. **118**, 217202 (2017).

[15] L. Lu, M. Song, W. Liu, A. P. Reyes, P. Kuhns, H. O. Lee, I. R. Fisher, and V. F. Mitrović, Nature Communications **8**, 14407 EP (2017).

[16] W. Liu, R. Cong, E. Garcia, A. Reyes, H. Lee, I. Fisher, and V. Mitrovi, Physica B: Condensed Matter **536**, 863 (2018).

[17] D. Hirai and Z. Hiroi, Journal of the Physical Society of Japan **88**, 064712 (2019).

[18] C. M. Thompson, J. P. Carlo, R. Flacau, T. Aharen, I. A. Leahy, J. R. Pollichemi, T. J. S. Munsie, T. Medina, G. M. Luke, J. Munevar, S. Cheung, T. Goko, Y. J. Uemura, and J. E. Greedan, Journal of Physics: Condensed Matter **26**, 306003 (2014).

[19] E. Kermarrec, C. A. Marjerrison, C. M. Thompson, D. D. Maharaj, K. Levin, S. Kroeker, G. E. Granroth, R. Flacau, Z. Yamani, J. E. Greedan, and B. D. Gaulin, Phys. Rev. B **91**, 075133 (2015).

[20] C. A. Marjerrison, C. M. Thompson, A. Z. Sharma, A. M. Hallas, M. N. Wilson, T. J. S. Munsie, R. Flacau, C. R. Wiebe, B. D. Gaulin, G. M. Luke, and J. E. Greedan, Phys. Rev. B **94**, 134429 (2016).

[21] P. Santini, S. Carretta, G. Amoretti, R. Caciuffo, N. Magnani, and G. H. Lander, Rev. Mod. Phys. **81**, 807 (2009).

[22] P. Santini and G. Amoretti, Phys. Rev. Lett. **85**, 2188 (2000).

[23] J. A. Paixão, C. Detlefs, M. J. Longfield, R. Caciuffo, P. Santini, N. Bernhoeft, J. Rebizant, and G. H. Lander, Phys. Rev. Lett. **89**, 187202 (2002).

[24] A. Kiss and P. Fazekas, Phys. Rev. B **68**, 174425 (2003).

[25] Y. Tokunaga, D. Aoki, Y. Homma, S. Kambe, H. Sakai, S. Ikeda, T. Fujimoto, R. E. Walstedt, H. Yasuoka, E. Yamamoto, A. Nakamura, and Y. Shiokawa, Phys. Rev. Lett. **97**, 257601 (2006).

[26] K. Haule and G. Kotliar, Nature Physics **5**, 796 EP (2009).

[27] H.-H. Kung, R. E. Baumbach, E. D. Bauer, V. K. Thorsmølle, W.-L. Zhang, K. Haule, J. A. Mydosh, and G. Blumberg, Science **347**, 1339 (2015).

[28] H.-H. Kung, S. Ran, N. Kanchanavatee, V. Krapivin, A. Lee, J. A. Mydosh, K. Haule, M. B. Maple, and G. Blumberg, Phys. Rev. Lett. **117**, 227601 (2016).

[29] A. Sakai and S. Nakatsuji, Journal of the Physical Society of Japan **80**, 063701 (2011).

[30] T. J. Sato, S. Ibuka, Y. Nambu, T. Yamazaki, T. Hong, A. Sakai, and S. Nakatsuji, Phys. Rev. B **86**, 184419 (2012).

[31] M. Tsujimoto, Y. Matsumoto, T. Tomita, A. Sakai, and S. Nakatsuji, Phys. Rev. Lett. **113**, 267001 (2014).

[32] L. Fu, Phys. Rev. Lett. **115**, 026401 (2015).

[33] J. W. Harter, Z. Y. Zhao, J.-Q. Yan, D. G. Mandrus, and D. Hsieh, Science **356**, 295 (2017).

[34] S. Hayami, H. Kusunose, and Y. Motome, Phys. Rev. B **97**, 024414 (2018).

[35] D. D. Maharaj, G. Sala, M. B. Stone, E. Kermarrec, C. Ritter, F. Fauth, C. A. Marjerrison, J. E. Greedan, A. Paramekanti, and B. D. Gaulin, "Supplemental material: Octupolar vs néel order in cubic $5d^2$ double perovskites," (2019), description: Part I: Experiment Details. Part IA. Time-of-flight inelastic neutron scattering. Part IB. High intensity neutron powder diffraction. Part IC. High angular resolution x-ray diffraction. Part II: Theory. Part IA. Single-site model, multipole moments.

[36] K. Yamamura, M. Wakeshima, and Y. Hinatsu, Journal of Solid State Chemistry **179**, 605 (2006).

[37] R. Morrow, A. E. Taylor, D. J. Singh, J. Xiong, S. Rodan, A. U. B. Wolter, S. Wurmehl, B. Büchner, M. B. Stone, A. I. Kolesnikov, A. A. Aczel, A. D. Christianson, and P. M. Woodward, Scientific Reports **6**, 32462 EP (2016).

[38] D. D. Maharaj, G. Sala, C. A. Marjerrison, M. B. Stone, J. E. Greedan, and B. D. Gaulin, Phys. Rev. B **98**, 104434 (2018).

[39] A. E. Taylor, R. Morrow, D. J. Singh, S. Calder, M. D. Lumsden, P. M. Woodward, and A. D. Christianson, Phys. Rev. B **91**, 100406 (2015).

[40] C. M. Thompson, C. A. Marjerrison, A. Z. Sharma, C. R. Wiebe, D. D. Maharaj, G. Sala, R. Flacau, A. M. Hallas, Y. Cai, B. D. Gaulin, G. M. Luke, and J. E. Greedan, Phys. Rev. B **93**, 014431 (2016).

[41] A. A. Aczel, D. E. Bugaris, L. Li, J.-Q. Yan, C. de la Cruz, H.-C. zur Loye, and S. E. Nagler, Phys. Rev. B **87**, 014435 (2013).

[42] J. Xiong, J. Yan, A. A. Aczel, and P. M. Woodward, Journal of Solid State Chemistry **258**, 762 (2018).

[43] R. T. Azuah, L. R. Kneller, Y. Qiu, P. L. W. Tregenna-Piggott, C. M. Brown, J. R. D. Copley, and R. M. Dimeo, J. Res. Natl. Inst. Stand. Technol. **114**, 341 (2009).

[44] O. Arnold, J. Bilheux, J. Borreguero, A. Buts, S. Campbell, L. Chapon, M. Doucet, N. Draper, R. F. Leal, M. Gigg, V. Lynch, A. Markvardsen, D. Mikkelson, R. Mikkelson, R. Miller, K. Palmen, P. Parker, G. Passos, T. Perring, P. Peterson, S. Ren, M. Reuter, A. Savici, J. Taylor, R. Taylor, R. Tolchenov, W. Zhou, and J. Zikovsky, Nuclear Instruments and Methods in Physics Research Section A: Accelerators, Spectrometers, Detectors and Associated Equipment **764**, 156 (2014).

[45] J. Rodriguez-Carvajal, Physica B **192**, 55 (1993).

[46] K. Kobayashi, T. Nagao, and M. Ito, Acta Crystallographica Section A **67**, 473 (2011).

[47] P. J. van der Linden, M. Moretti Sala, C. Henriquet, M. Rossi, F. Ohgushi, K. Fauth, L. Simonelli, C. Marini, E. Fraga, C. Murray, J. Potter, and M. Krisch, Rev. Sci. Instrum. **87**, 115103 (2016).

[48] T. C. Hansen, P. F. Henry, H. E. Fischer, J. Torregrossa, and P. Convert, Measurement Science and Technology **19**, 034001 (2008).

[49] G. E. Granroth, A. I. Kolesnikov, T. E. Sherline, J. P. Clancy, K. A. Ross, J. P. C. Ruff, B. D. Gaulin, and S. E. Nagler, Journal of Physics: Conference Series **251**, 012058 (2010).

[50] J. P. Carlo, J. P. Clancy, K. Fritsch, C. A. Marjerrison, G. E. Granroth, J. E. Greedan, H. A. Dabkowska, and B. D. Gaulin, Phys. Rev. B **88**, 024418 (2013).

[51] F. Fauth, I. Peral, C. Popescu, and M. Knapp, Powder Diffr. **28**, S360 (2013).

[52] W. Liu, R. Cong, A. P. Reyes, I. R. Fisher, and V. F. Mitrović, Phys. Rev. B **97**, 224103 (2018).

[53] A. Paramekanti, D. D. Maharaj, and B. D. Gaulin, (2019), arXiv:1909.03089 [cond-mat.str-el].

[54] A. S. Patri, A. Sakai, S. Lee, A. Paramekanti, S. Nakatsuji, and Y. B. Kim, arXiv e-prints , arXiv:1901.00012 (2018), arXiv:1901.00012 [cond-mat.str-el].